Reaction of SO_2 with Cesium and Cesium-Promoted ZnO and MoO_2

José A. Rodriguez,* Tomas Jirsak, and Jan Hrbek

Department of Chemistry, Brookhaven National Laboratory, Upton, New York 11973

Received: November 5, 1998; In Final Form: January 16, 1999

The chemistry of SO_2 on pure metallic Cs and Cs-promoted polycrystalline surfaces of ZnO and MoO_2 has been studied using high-resolution synchrotron-based photoemission. Metallic cesium reacts vigorously with SO_2 at temperatures between 100 and 300 K. At 100 K, the amount of SO_2 that fully dissociates ($SO_{2,gas} \rightarrow S_a + 2O_a$) on the alkali metal is relatively small, and SO_x ($x = 2-4$) species predominate on the surface. SO_3 and SO_4 may be formed as a result of the reaction of SO_2 with atomic oxygen ($SO_2 + nO_a \rightarrow SO_{2+n,a}$ where $n = 1-2$), or by disproportionation of chemisorbed SO_2. At 300 K the stability of the $CsSO_x$ species is lower than at 100 K, and the formation of CsO_y and CsS_y becomes important. In the Cs/ZnO and Cs/MoO_2 systems, the alkali ↔ oxide interactions are very strong. Despite this, the supported Cs atoms retain a large chemical affinity for SO_2 and are able to enhance the rate of adsorption of the molecule on the oxide surfaces, even at low coverages (0.1−0.2 ML) of cesium when the alkali atoms are in a highly ionic state ($Cs^{\delta+}$). The larger the coverage of Cs on ZnO and MoO_2, the faster the rate of adsorption of SO_2, and the larger the amount of S and SO_x ($x = 2-4$) species present on the surface. The adsorption of SO_2 on ZnO and Cs/ZnO surfaces was examined using ab initio self-consistent-field (SCF) calculations and cluster models. The Cs adatoms provide occupied states that are very efficient for bonding interactions with the LUMO of SO_2. Cs atoms supported on Zn-terminated terraces of ZnO respond much more strongly to the presence of SO_2 than Cs atoms supported on O-terminated terraces. The bonding interactions between the ZnO(0001)−Zn face and SO_2 are weak, and promotion with Cs adatoms considerably improves the energetics for SO_2 adsorption.

1. Introduction

Sulfur-containing molecules are common impurities present in coal and crude oil. Sulfur dioxide (SO_2) is a major air pollutant produced by the combustion of coal and fuels derived from petroleum.[1] In the atmosphere, SO_2 is oxidized and interacts with water to produce acid rain that kills vegetation and corrodes buildings and monuments.[1] In addition, SO_2 poisons the catalysts that are used for the removal of CO and NO from automobile exhaust ($2CO + O_2 \rightarrow 2CO_2$; $2CO + 2NO \rightarrow 2CO_2 + N_2$).[2] Thus, from a practical viewpoint, it is important to have a fundamental understanding of the factors that determine the behavior of SO_2 on metal and oxide surfaces. This fundamental knowledge can be useful for controlling corrosion processes and sulfur poisoning, and for the design of catalysts that are highly active for the conversion or destruction of SO_2.

Many recent studies have focused their attention on the interaction of SO_2 with transition-metal single crystals.[3−10] These studies have shown that sulfur dioxide decomposes either spontaneously or by thermal activation in all the metal substrates studied so far (Fe, Ni, Cu, Mo, Ru, Rh, Pd, Pt) except Ag, where it adsorbs molecularly.[3n,6] A comparison of the behavior of SO_2 on Mo(110),[9] Ru(001),[7] Rh(111),[10] and Pt(111)[8] shows that the reactivity of the metals toward the molecule increases following the sequence: Pt ≈ Rh < Ru < Mo. The bonding interactions between SO_2 and a metal are dominated by a transfer of electrons from the metal into the LUMO of SO_2 ($3b_1$ orbital).[6,8,11,12] Bimetallic bonding can induce a redistribution of electrons around a metal center, reducing its ability to respond to the presence of SO_2.[8,10] In the Sn/Pt(111) system, a tin-induced decrease in the d electron density of Pt leads to a reduction in the reactivity of this metal toward SO_2[8] and other sulfur-containing molecules.[13] A similar phenomenon is seen after bonding Pd to Rh(111) or surfaces of early-transition metals.[10] In principle, bimetallic bonding can be useful for increasing the sulfur tolerance of metal catalysts (i.e., controlling sulfur poisoning).[8,10,13,14]

Sorbents or catalysts based on metal oxides offer a convenient route for the removal or destruction of sulfur oxides (DeSO*x* process).[1b,15−20] This fact has spawned much interest in the chemistry of SO_2 on well-defined surfaces of metal oxides: TiO_2,[21] Ti_2O_3,[22] Fe_2O_3,[23] V_2O_3,[24] V_2O_5,[25] NiO,[26] ZnO,[27] Al_2O_3,[18,28] and MgO.[12,29] In general, these systems exhibit a very low reactivity toward SO_2, and only when defect sites are present on the surface, does one see significant interactions between the metal oxide and the molecule. A series of adsorbed species (S, SO, SO_3, and SO_4) have been proposed as intermediates and products of the reaction with SO_2. Sulfur dioxide mainly interacts with the O centers of the oxides.[12,18,29]

Little is known about the behavior of SO_2 on surfaces of pure alkali metals. However, it is well-established that the activity of an oxide catalyst or sorbent in the DeSO*x* process can be enhanced by addition of an alkali metal.[18−20] In general, the DeSO*x* catalysts or sorbents are complex systems and the exact role of the alkali in the removal process is poorly understood. The alkali may be the real active phase or "simply" a promoter of the chemical activity of the oxide substrate. The electronic interactions between an alkali metal and an oxide can be very strong,[30,31] opening the possibility for large changes in the chemical properties of both components. In this article, we use high-resolution synchrotron-based photoemission to study the

* Corresponding author. Fax: 516-344-5815. E-mail: rodrigez@bnl.gov.

10.1021/jp984318d CCC: $18.00
Published on Web 03/02/1999

reaction of SO_2 with pure polycrystalline cesium and cesium-promoted surfaces of ZnO and MoO_2. The adsorption of SO_2 on Cs/ZnO(0001)−Zn and Cs/ZnO(000$\bar{1}$)−O is examined using ab initio self-consistent-field (SCF) calculations. These studies reveal a rich and interesting surface chemistry that depends strongly on coverage and temperature.

2. Experimental and Theoretical Methods

2.1. Synchrotron Core-Level and Valence-Band Data. The experiments were carried out in an ultrahigh-vacuum (UHV) chamber that is part of the U7A beamline at the National Synchrotron Light Source (NSLS) at Brookhaven National Laboratory. The UHV chamber is equipped with a hemispherical electron energy analyzer with multichannel detection, a Mg Kα X-ray source, and a quadrupole mass spectrometer. The valence and S 2p spectra were acquired using the beam at a photon energy of 260 eV, whereas Mg Kα radiation was used to take the Cs 3d and O 1s spectra. The binding energy in the S 2p and valence spectra was calibrated by the position of the Fermi edge. In the experiments with X-ray photoelectron spectroscopy (XPS), the binding energy scale was established by setting the Cs $3d_{5/2}$ peak of a thick Cs multilayer at a binding energy of 726.6 eV.[32]

Films of polycrystalline Cs, ZnO, and MoO_2 were grown on a Mo(110) substrate. A standard procedure was applied to clean the Mo crystal.[9] Ultrathin oxide films have emerged as a convenient way to study the chemical properties of oxide surfaces.[33,34] In this work, films of ZnO (>10 layers in thickness) were grown on a Mo(110) substrate using procedures described elsewhere.[35−37] Following this methodology one gets quasi layer-by-layer growth, and the films of zinc oxide are polycrystalline with electronic properties and a phonon structure that are identical to those of bulk ZnO.[35−37] MoO_2 films (5−6 layers in thickness) were grown using a literature protocol in which Mo(110) was oxidized under 3×10^{-5} Torr of O_2 for 5 min at 1050 K.[38]

Multilayers of cesium (8−10 layers) were vapor deposited on Mo(110) at 100 K, whereas submonolayer coverages of the alkali were vapor-deposited on ZnO and MoO_2 at 300 K. The evaporation of Cs was achieved by heating a SAES getter chromate source. For small doses, the relative coverage of Cs was determined by comparing the area under the Cs $3d_{5/2}$ XPS peak to the corresponding area for a full layer of chemisorbed Cs on Mo(110) at 300 K, which has an absolute coverage of $5.1-5.2 \times 10^{14}$ Cs adatoms cm^{-2}.[39]

High-purity sulfur dioxide (Mattheson) was dosed to the Cs, Cs/ZnO, and Cs/MoO_2 surfaces from the background by backfilling the UHV chamber. The purity of the SO_2 doses was confirmed using a mass spectrometer. The coverage of sulfur on the surfaces was determined by measuring the area under the S 2p features, which was scaled to absolute values by comparing it to the corresponding area for the saturation coverage of atomic S on Mo(110) known to be 0.91 monolayer (ML).[40] In this work, the coverages of S and Cs are reported with respect to the number of Mo(110) surface atoms, i.e., 1.43×10^{15} adatoms cm^{-2} corresponds to $\theta = 1$ ML.

2.2. Molecular Orbital Calculations. The ab initio SCF calculations described in section 3.2 for the adsorption of SO_2 on Cs/ZnO clusters were performed using the HONDO program.[41] The molecular orbitals were expanded using Gaussian-type orbitals (GTOs). For the S and O atoms in SO_2, we included all their electrons in the calculations. The atomic orbitals of these atoms were expressed in terms of double-ζ quality basis sets augmented with polarization functions.[8,27,35,42] Since the systems under consideration contain a large number of heavy atoms, the nonempirical effective core potentials of Hay and Wadt[43] were used to describe the inner shells of Zn and Cs. A basis set obtained through a (3s3p5d/2s1p2d) contraction scheme[27,35,42,44] was employed to describe the 4s, 4p, and 3d valence orbitals of zinc. The 6s and 6p atomic orbitals of cesium were described in terms of a (3s3p/1s1p) basis set.[42a,43b] Most of the oxygen atoms in the ZnO clusters were treated using the effective core potential (1s shell) and orbital basis set (2s,2p shells) recommended by Stevens, Basch, and Krauss.[45] The only exception was the oxygen atoms to which SO_2 and Cs were bonded. For these O atoms, we included all its electrons in the calculations and the atomic orbitals were expressed using the same basis set employed to describe the oxygens in the SO_2 molecule.

Previous experience[8,9,35,42] indicates that the type of ab initio SCF calculations performed here give satisfactory adsorption geometries but underestimate adsorption energies. Due to the approximations of our theoretical approach (size of the basis set, lack of electron correlation, use of finite clusters), the energetics derived from these SCF calculations simply provides a guide for the interpretation of experimental results.[8,9,35,42] The use of ab initio SCF methods with cluster models has proved to be a very useful approach for studying a large variety of phenomena that occur on surfaces of metals and oxides.[34,46,47]

3. Results

3.1. Interaction of SO_2 with Metallic Cesium. Figure 1 shows S 2p and valence spectra acquired after successive doses of SO_2 to a polycrystalline film of cesium (8−10 layers) at 100 K, and subsequent annealing to 200 and 300 K. A small SO_2 dose of 0.1 L produces weak features between 161 and 162 eV, and between 6 and 8 eV that indicate the presence of atomic S[42a,48] and O[49] yielded by the complete dissociation of sulfur dioxide ($SO_2 \rightarrow S_a + 2O_a$). After an additional SO_2 dose of 0.2 L, the S 2p features for molecular SO_x species begin to appear between 166 and 168 eV.[8−10,50] These features eventually dominate the S 2p region when the exposure of SO_2 is increased. Upon a total dose of 2.3 L of SO_2, the valence region displays peaks for the O 2p and S 3p orbitals of atomic species (3.5 and 6.5 eV)[48,49] plus peaks for molecular orbitals of SO_x species (9, 11, and 13 eV).[4e,k] Heating from 100 to 200 K induces the desorption or reaction of the physisorbed SO_2,[8−10] and drastic changes are observed in the line shape of the S 2p and valence regions. There is a shift of ∼ 0.6 eV toward lower binding energy in all the photoemission peaks. An identical shift was found in the Cs 3d levels (see below). Such a behavior, which has also been observed for the O_2/Cs system,[51] suggests the occurrence of a phase transition or transformation that shifts the position of the Fermi edge for the film.[52] After heating to 200 K, one sees a substantial increase in the photoemission peaks for atomic S and O (∼161 and 5.4 eV).[42a,48,49] The S 2p features between 165 and 170 eV are well fitted[48,53] by a set of two doublets that can be assigned to SO_2 and SO_4 species bonded to cesium.[8−10,50] Further heating to 300 K leads to a decrease in the intensity of the S 2p features for SO_2 and SO_4 and no significant change in the peaks for atomic S and O. At room temperature, the cesium atoms are bonded to SO_4, SO_2, S, and/or O.

Figure 2 displays XPS data acquired in the same set of experiments that produced the photoemission spectra in Figure 1. In the Cs 3d spectrum for the pure Cs multilayer (top panel), the two sharp features at 726.6 and 740.5 eV are the main levels whereas the broad shoulders toward higher binding energy

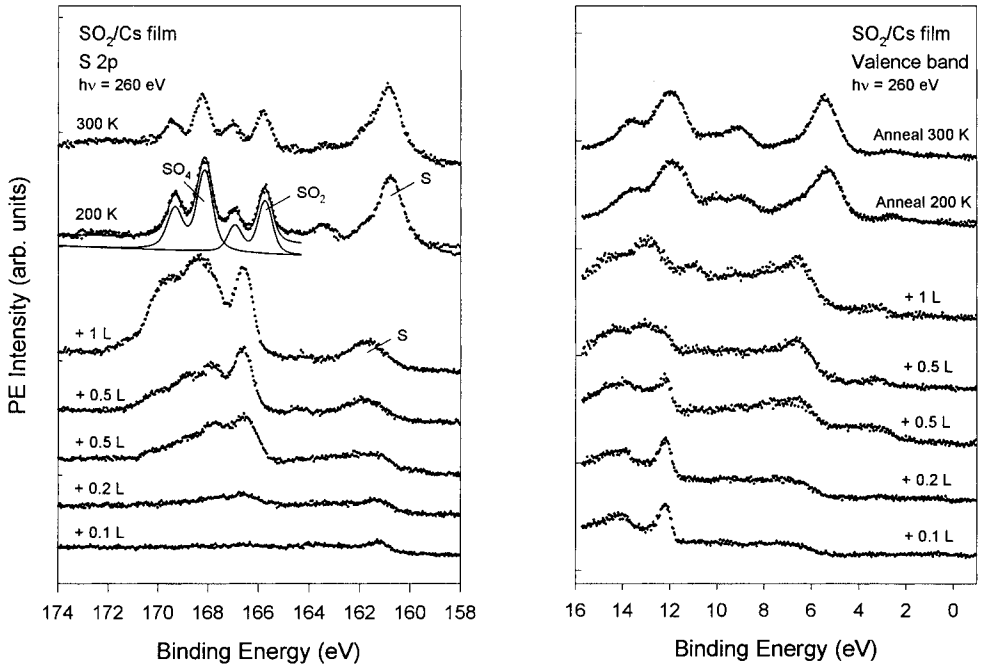

Figure 1. S 2p (left) and valence (right) spectra for the interaction of SO_2 with a polycrystalline film of cesium. The dosing of sulfur dioxide (0.1, 0.2, 0.5, 0.5, and 1 L) was carried out at 100 K. Then, the sample was heated to 200 and 300 K. A photon energy of 260 eV was used to excite the electrons in these experiments. The S 2p spectrum obtained after heating to 200 K was curve-fitted following the procedure described in refs 48 and 53.

correspond to plasmon losses.[51] The reaction with SO_2 leads to a decrease in the magnitude of the plasmon losses, with the main 3d levels gaining intensity. This behavior is identical to that observed after exposing metallic cesium to O_2[51] or S_2.[42a] At this point the corresponding O 1s spectrum (at the bottom of Figure 2) displays a very broad peak that contains contributions from physisorbed SO_2,[8,9,27] plus oxygen[51] and SO_x species[8,9,27] bonded to cesium. Heating from 100 to 200 K induces a substantial transformation in the film and all the photoemission peaks shift toward lower binding energy (compare to S 2p and valence data in Figure 1). In the O 1s region, one sees a drastic drop in the intensity of the features that appear above 533 eV and are due to physisorbed SO_2.[8,9,27] At the same time, there is a gain in the signal around 530−531 eV where CsO_x appears.[51]

In summary, it was found that an alkali metal such as Cs is very reactive toward SO_2 at temperatures between 100 and 300 K. At 100 K, the amount of SO_2 that fully dissociates ($SO_{2,gas} \rightarrow S_a + 2O_a$) on the alkali metal is relatively small, and SO_x species predominate on the surface. SO_3 and SO_4 may be formed as a result of the reaction of SO_2 with atomic oxygen[8−10]

$$SO_2 + nO_a \rightarrow SO_{2+n,a} \qquad n = 1-2 \qquad (1)$$

or by disproportionation of chemisorbed SO_2[8,27]

$$mSO_{2,a} \rightarrow (m-1)SO_{gas} + SO_{1+m,a} \qquad m = 2-3 \qquad (2)$$

At room temperature, the stability of the $CsSO_x$ species is lower than at 100 K, and the formation of CsO_x and CsS_x becomes important.

3.2. Interaction of SO_2 with ZnO and Cs/ZnO Surfaces. Figure 3 shows S 2p spectra obtained after successive doses of SO_2 to polycrystalline ZnO at 300 K. The type of oxide surfaces examined in this work exposed approximately a 50:50 mixture of Zn and O.[27,35,37,42a] Our previous studies have shown that the zinc sites of these surfaces are reactive toward sulfur-containing molecules.[27,37,42a] In Figure 3, even at the lowest SO_2 exposure, one sees only a broad feature centered at ∼167.5 eV which corresponds to the formation of SO_4 species.[8−10,27]. This feature grows in intensity with increasing SO_2 exposure, and no signal is seen for SO_2 or S bonded to zinc sites.[27] Similar experiments on polycrystalline Zn mainly led to the full decomposition of SO_2 and the formation of ZnS_x and ZnO_x.[27] On zinc oxide, SO_4 can be formed through a reaction of SO_2 with O sites (eq 1) or by disproportionation of chemisorbed SO_2 on Zn sites (eq 2). The second possibility is highly unlikely because no Zn-bonded SO_2 or S species are seen in photoemission. The results of Figure 3 indicate that SO_2 preferentially reacts with O sites of the oxide and more or less ignores the Zn sites (the formed SO_4, however, does interact with the Zn sites). After an SO_2 exposure of 1.8 L, the ZnO is covered with a SO_4 layer that has a sulfur coverage of ∼0.6 ML. When the system was annealed to 500 K, the S 2p peaks became more well-defined without any appreciable change in intensity. Most of the SO_4 species disappeared after heating to 700 K, leaving mainly chemisorbed S on the Zn sites of the oxide surface (not shown).

The interaction of cesium with polycrystalline ZnO was examined in detail in a previous work.[54] At small Cs coverages, $\theta_{Cs} < 0.2$ ML, cesium forms very strong adsorption bonds on polycrystalline ZnO with desorption temperatures higher than 700 K. The strength of the Cs−ZnO bond depends on the coverage of cesium, and for a saturated adlayer ($\theta_{Cs} \approx 0.6$ ML) the desorption of the alkali starts around 300 K.[54] These trends are similar to those found in thermal-desorption spectra for Cs/TiO_2[55] and Cs/Al_2O_3,[56] where the alkali desorbs in a broad range of temperatures. This phenomenon has been attributed to a reduction in the ionicity of the Cs−ZnO bond with increasing Cs coverage[54] due to dipole−dipole repulsion.[30,31] At low coverages, the cesium adatoms are in a highly ionic state but they are not fully oxidized ($Cs^{\delta+}$).[54]

Figure 4 displays S 2p spectra for the adsorption of SO_2 on two different Cs/ZnO systems at 300 K. The data in the left-side panel is for a surface with a full layer of chemisorbed

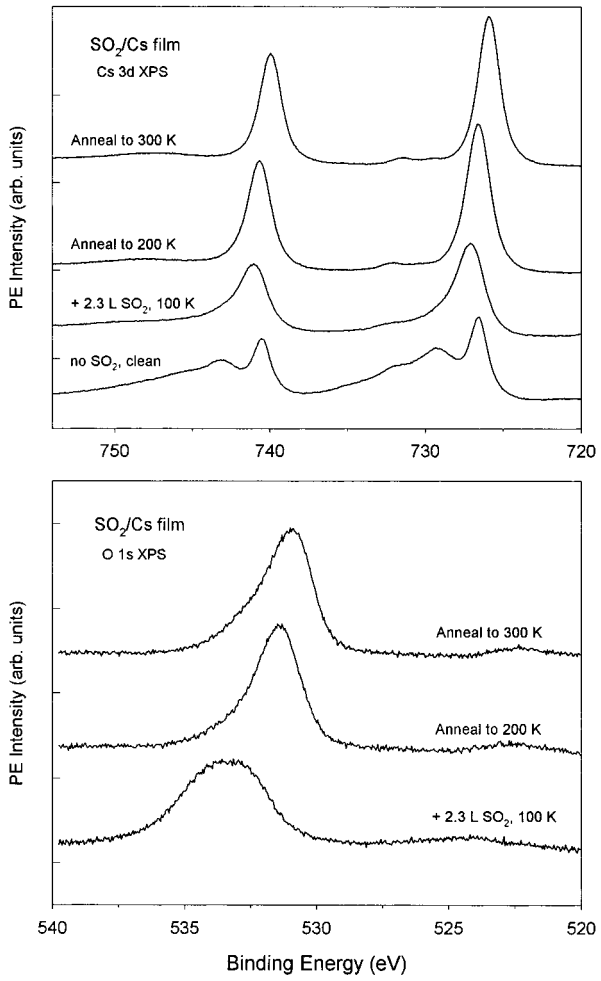

Figure 2. Cs 3d (top panel) and O 1s (bottom panel) XPS spectra for the reaction of SO_2 with metallic cesium at 100 K and subsequent annealing to 200 and 300 K. The spectra were acquired using Mg Kα radiation.

cesium ($\theta_{Cs} = 0.6$ ML, $Cs_{0.6}$/ZnO), whereas the data in the right-side panel is for a surface partially covered with the alkali ($\theta_{Cs} = 0.25$ ML, $Cs_{0.25}$/ZnO). In general, Cs adatoms enhance the reactivity of ZnO surfaces toward SO_2. On the $Cs_{0.6}$/ZnO system, the first dose of SO_2 produces only an ill-defined peak at ~161 eV that can be assigned to atomic S bonded to cesium.[42a] As the doses of SO_2 increase, two extra doublets appear in the S 2p region that correspond to SO_2 ($2p_{3/2}$ peak at 165.3 eV)[8−10,50] and SO_4 ($2p_{3/2}$ peak at 167.8 eV)[8−10,50]. The S, SO_2, and SO_4 are probably bonded to the cesium overlayer. After a total exposure of 1.5 L, the features for SO_4 dominate the S 2p region. The corresponding O 1s spectrum (bottom panel in Figure 5) exhibits a very broad peak that contains contributions from at least two types of oxygen species. The O 1s features toward higher binding energy denote the presence of SO_4 on the surface.[27] Heating from 300 to 500 K induces the desorption or decomposition of a large fraction of the adsorbed SO_4. In the S 2p region (left panel in Figure 4) the signal for atomic S gains intensity. A strong peak appears at 162.3 eV that can be attributed to S bonded to Zn sites of ZnO.[35] The heating led to desorption of part of the cesium (see top panel in Figure 5) and probably a change in the morphology of the overlayer that uncovered regions of the ZnO substrate. Additional heating to 710 K induced the desorption of most of the Cs (Figure 5), and the SO_4 almost disappeared from the surface (Figure 4). At this point, the S 2p spectrum was dominated by a peak for S bonded to Zn sites of ZnO.

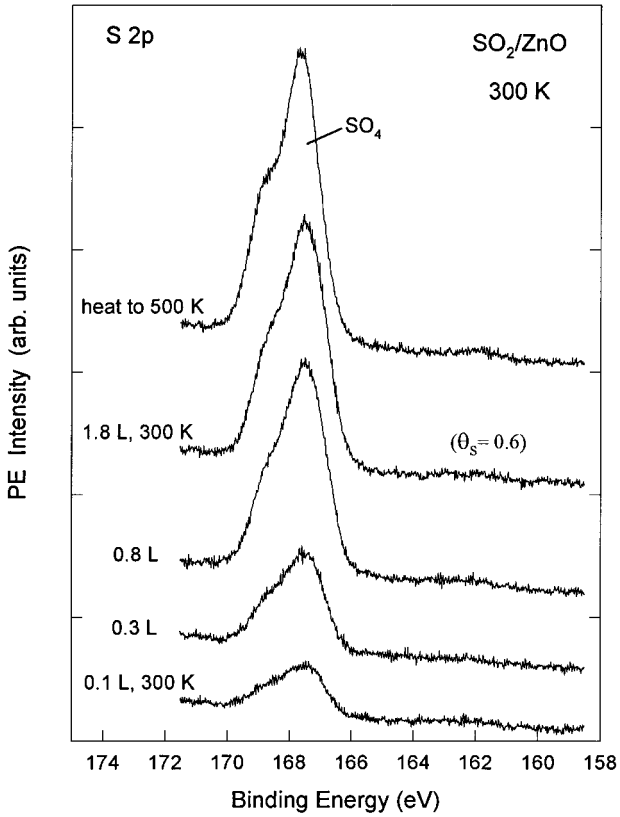

Figure 3. S 2p spectra for the SO_2/ZnO system as a function of SO_2 exposure. SO_2 was dosed at 300 K, and in the final step the surface was annealed to 500 K. All the spectra were taken using a photon energy of 260 eV.

The results for the adsorption of SO_2 on $Cs_{0.25}$/ZnO (right-side panel in Figure 4) show trends that are very similar to those seen for the adsorption of SO_2 on $Cs_{0.6}$/ZnO. In the $Cs_{0.25}$/ZnO system, most of the surface is not covered by cesium and this admetal is in a partially ionic state ($Cs^{\delta+}$).[54] Here, one can compare the relative reactivity of the oxide and alkali sites toward SO_2. A small dose of 0.1 L of SO_2 produces S 2p features for atomic S (~161 eV), SO_2 (~165.8 eV), and SO_4 (~168 eV). The S and SO_2 are bonded to Cs (see section 3.1), whereas the SO_4 may be associated with the alkali or oxide substrate. By comparing the relative intensity of the S 2p features, it is clear that SO_2 prefers to react or interact with the supported alkali. An increase in the SO_2 doses produces mainly SO_4, and features for S bonded to Zn sites appear between 164 and 162 eV.[35] When the temperature is raised from 300 to 650 K, the S 2p signal for SO_4 decreases and the signal for Zn-bonded S increases.

By comparing the results for the interaction of SO_2 with ZnO (Figure 3) and Cs/ZnO (Figure 4), one can notice important differences. On ZnO, the adsorption of SO_2 does not lead to the presence of S and SO_2 on the surface at 300 K. On ZnO the main interaction of SO_2 is with the O sites (SO_4 formation), whereas on Cs/ZnO the molecule mainly reacts with the metal adatoms or with adsorption sites that involve Cs and O. The larger the coverage of Cs on ZnO, the faster the rate of adsorption of SO_2 and the larger the amount of atomic S and SO_x ($x = 2-4$) formed. The Cs atoms supported on zinc oxide exhibit a chemistry as complex as that found for pure metallic cesium (coexistence of S, SO_2, and SO_4).

The bonding of SO_2 to ZnO and Cs/ZnO was examined using ab initio SCF calculations and cluster models. Figure 6 shows the $Zn_{13}O_{13}$ cluster that was used to represent (0001)−Zn and

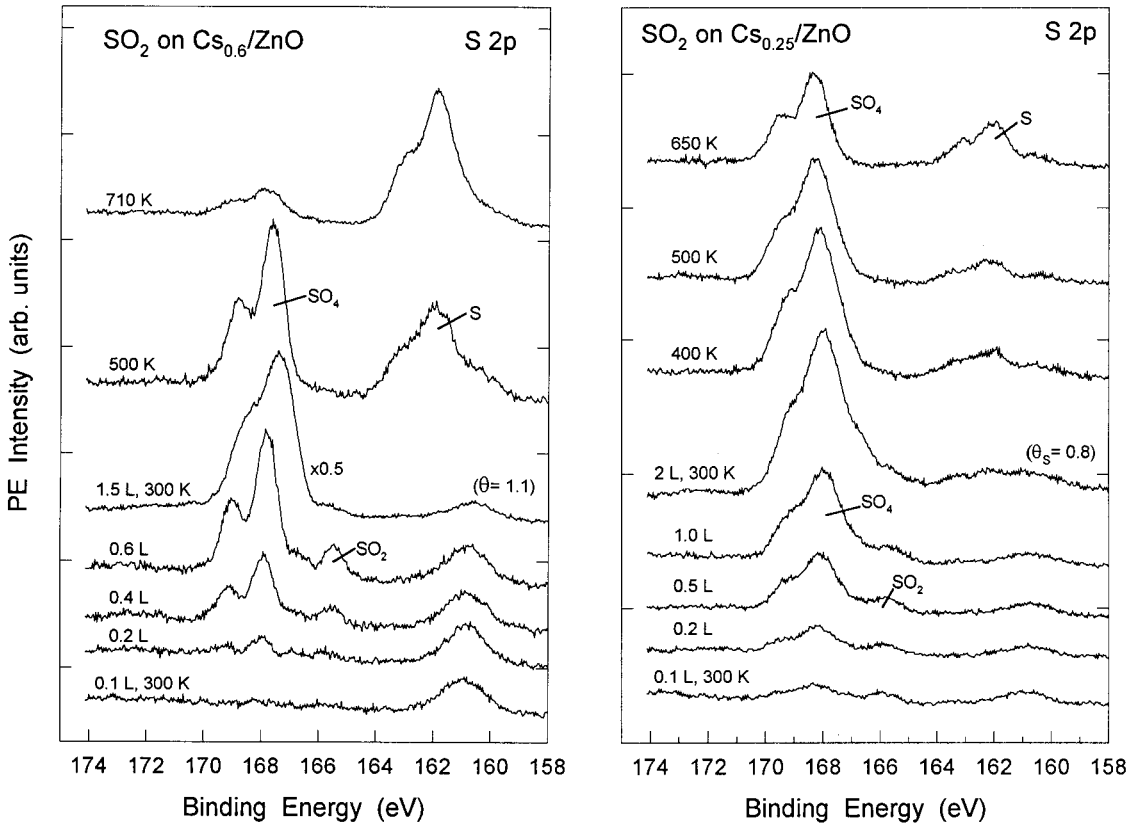

Figure 4. Left panel: S 2p spectra for the adsorption of SO_2 on a ZnO surface precovered with 0.6 ML of Cs. First, $Cs_{0.6}$/ZnO was exposed to five different doses of SO_2 (the reported values in the figure are for total exposures) at 300 K. Then, the final $SO_2/Cs_{0.6}$/ZnO system was heated to 500 and 710 K. Right panel: Similar S 2p data for the adsorption of SO_2 on a ZnO surface precovered with 0.25 ML of Cs. SO_2 was dosed at 300 K, followed by annealing to 400, 500, and 650 K. All the spectra were acquired using a photon energy of 260 eV.

$(000\bar{1})$−O terraces of zinc oxide. Previous studies have shown that clusters of this size provide the basic physical and chemical interactions that are responsible for the bonding of small molecules to zinc oxide surfaces.[27,35,42a,57] The $Zn_{13}O_{13}$ cluster has four layers arranged in the structural geometry of bulk ZnO.[58] The first and third layers are entirely zinc, and the second and fourth are oxygen layers. The first layer is a model for the ZnO(0001)−Zn surface, while the fourth layer represents the ZnO $(000\bar{1})$−O surface. To model supported cesium, a Cs atom was set on the center of the hollow site formed by the Zn atoms labeled 1 in the first layer {$Cs/Zn_{13}O_{13}$(0001) configuration}, or the center of the hollow site formed by the O atoms labeled 1′ in the fourth layer {$Cs/Zn_{13}O_{13}(000\bar{1})$ configuration}. Estimates based on pure electrostatic interactions and a Madelung potential predict that these should be the adsorption sites of Cs on ZnO(0001)−Zn and ZnO$(000\bar{1})$−O.[59] In the case of K/ZnO-$(000\bar{1})$−O, SEXAFS indicates that potassium adsorbs on the 3-fold hollow sites of the O-terminated surface that have a Zn atom underneath.[60] In the present $Cs/Zn_{13}O_{13}$(0001) and $Cs/Zn_{13}O_{13}(000\bar{1})$ models, the Cs−Zn_1 and Cs−O_1 bond distances were optimized at the ab initio SCF level obtaining values of 3.32 and 2.97 Å (respectively). The calculations predict that cesium behaves as an electron donor on the (0001)−Zn and $(000\bar{1})$−O faces of zinc oxide. On the O-terminated surface the calculated positive charge[61] on the Cs adatom was 0.29 *e* larger than on the Zn-terminated surface. The charges on the Cs adatom have a marked effect on its reactivity toward SO_2 molecules as will be seen bellow.

Table 1 lists the structural parameters and bonding energies calculated for the adsorption of SO_2 on the $Zn_{13}O_{13}$(0001), $Cs/Zn_{13}O_{13}$(0001), $Zn_{13}O_{13}(000\bar{1})$, and $Cs/Zn_{13}O_{13}$ $(000\bar{1})$ systems. The molecule was bonded with the η^1-S and η^2-O,O configurations shown in Figure 6. On metal centers (Zn or Cs) di-coordination via oxygen is more stable than mono-coordination via S. This agrees well with trends seen in previous theoretical studies for the adsorption of SO_2 on metal surfaces.[7,8,62,63] When comparing the results for $Zn_{13}O_{13}$(0001)−Zn and $Zn_{13}O_{13}(000\bar{1})$−O, one finds that the O ↔ SO_2 bonding interactions are much stronger than the Zn ↔ SO_2 bonding interactions, in agreement with the experimental trends seen in Figure 3 where SO_2 preferentially reacts with O sites of polycrystalline ZnO. On $Zn_{13}O_{13}(000\bar{1})$−O, the molecule was bonded via S to an O atom labeled 1′ in Figure 6. After this adsorption geometry was optimized, the molecular plane of SO_2 was perpendicular to the $(000\bar{1})$−O surface. This bonding conformation produced a SO_3-like species that is the precursor for the abstraction of one O atom from ZnO and the formation of SO_4. This process cannot be modeled using the $Zn_{13}O_{13}$ cluster, but it can be expected in zinc oxide surfaces because $ZnSO_4$ ($\Delta H_f = -235$ kcal/mol)[64] is much more stable than ZnO ($\Delta H_f = -83$ kcal/mol).[64] After adding a Cs atom to the $Zn_{13}O_{13}$-$(000\bar{1})$−O surface, the adsorption energy of SO_2 on a $O_{1'}$ atom increased from 28 to 34 kcal/mol. Cs atoms supported on the (0001)−Zn and $(000\bar{1})$−O faces of the $Zn_{13}O_{13}$ cluster bond SO_2 much stronger than the metal centers in the (0001)−Zn face. Adsorption on the Zn sites leads to minor changes in the structural geometry of SO_2, whereas on the Cs adatoms there is a substantial elongation in the S−O bonds (0.05−0.11 Å) and an opening of the O−S−O angle (2−6°). Cs atoms supported on Zn sites of the oxide are probably responsible for the dissociation of SO_2 in the systems of Figure 4.

SO_2 has a large electron affinity (∼1.1 eV)[65] and behaves as an electron acceptor when bonded to metals.[6,8,11,12,66] The interactions between the LUMO of SO_2 ($3b_1$ orbital) and the

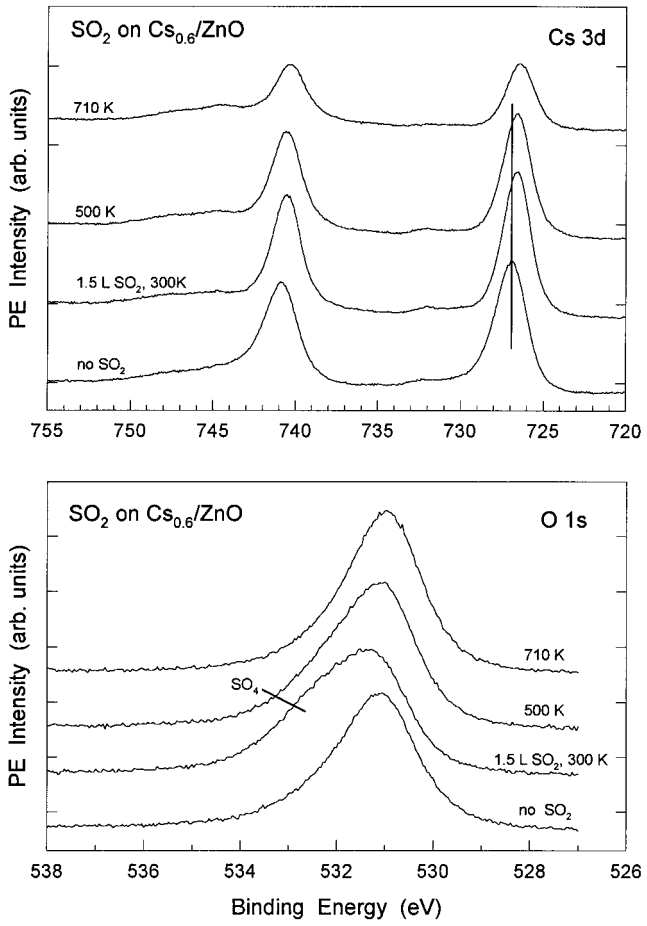

Figure 5. Cs 3d (top) and O 1s (bottom) XPS spectra for the reaction of SO_2 with a ZnO surface precovered with 0.6 ML of cesium. 1.5 L of SO_2 were dosed at 300 K and this was followed by heating to 500 and 710 K. The electrons were excited using Mg Kα radiation.

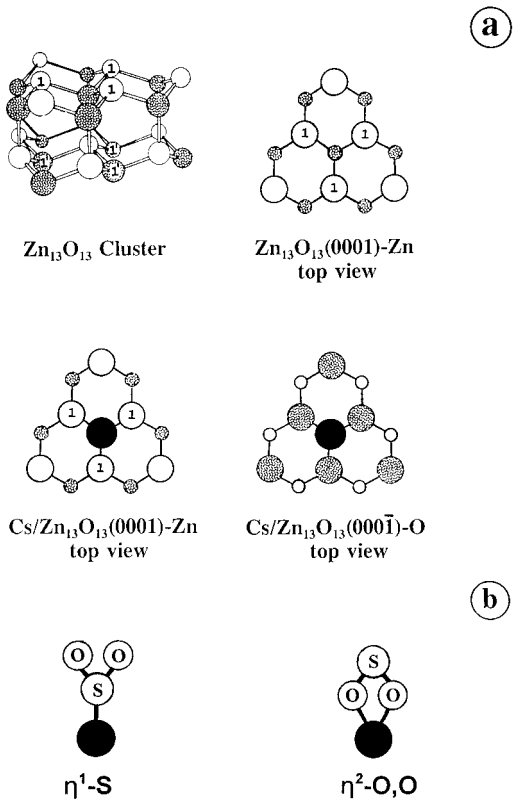

Figure 6. (a) Cluster used to model the adsorption of SO_2 on ZnO and Cs/ZnO surfaces. The cluster has 13 zinc atoms (empty circles) and 13 oxygen atoms (shaded circles) arranged in four layers with the geometry reported for the bulk oxide.[58] The (0001)−Zn and (000$\bar{1}$)−O faces of zinc oxide are represented by the first and four layers, respectively. A Cs atom was set directly above the hollow site formed by the Zn_1 atoms in the first layer {$Cs/Zn_{13}O_{13}(0001)$ configuration}, or above the hollow site formed by the $O_{1'}$ atoms in the fourth layer {$Cs/Zn_{13}O_{13}(000\bar{1})$ configuration}. (b) Bonding geometries for the adsorption of SO_2 on Zn and Cs atoms of ZnO and Cs/ZnO. The molecular plane of SO_2 was parallel to the surface normal.

occupied orbitals of the metal play a predominant role in the energetics of the metal−SO_2 bond.[11,12] In principle, any element that enhances the electron-donor ability of a surface should promote its chemical affinity for SO_2. Figure 7 shows the energy positions for the bands of bulk ZnO,[67] the 6s orbital of atomic Cs,[68] and the molecular orbitals of SO_2. For ZnO the empty and occupied bands are indicated by dotted and solid lines, respectively. The Cs 6s orbital is only partially occupied and gets stabilized (1.8−2.3 eV)[69] after interacting with zinc oxide. Following a simple model based on orbital mixing and a combination of perturbation theory with the Hückel or tight-binding method,[70,71] one can obtain an approximate expression for the bonding energy (Q) derived from the interaction between the LUMO of SO_2 and the valence band of ZnO (see Figure 7):

$$Q_{\mathrm{LUMO-Valence}} \propto \beta^2_{\mathrm{LUMO-Valence}}/(E_{\mathrm{LUMO}} - E_{\mathrm{valence}}) \quad (3)$$

Here, $\beta_{\mathrm{LUMO-Valence}}$ is a resonance integral for the interacting levels, E_{valence} is the energy for the centroid of the valence band of the oxide, and E_{LUMO} is the energy for the LUMO of SO_2. If one replaces E_{valence} with the energy for the Cs 6s orbital in eq 3, one can expect a big enhancement in the bonding interactions of SO_2 with the surface. This is consistent with the trends seen in the experimental data of Figures 3 and 4, and with the theoretical results listed in Table 1. The ab initio SCF calculations indicate that in the $Cs/Zn_{13}O_{13}(0001)$ system the Cs 6s orbital has a larger electron population and a lower stability than the Cs 6s orbital in $Cs/Zn_{13}O_{13}(000\bar{1})$.[69] Thus, according to perturbation theory,[70,71] a Cs atom supported on Zn-terminated terraces of ZnO should be able to respond more strongly to the presence of SO_2 than a Cs atom supported on O-terminated terraces. This line of thought agrees well with the ab initio SCF results reported in Table 1.

3.3. Interaction of SO_2 with MoO_2 and Cs/MoO_2 Surfaces. Our previous studies indicate that Mo(110) is very reactive toward SO_2.[9] At 300 K sulfur dioxide completely decomposes on the Mo(110) surface, and a SO_2 exposure of 4L produces a S saturation coverage of 0.36 ML.[9] Upon dosing at 100 K, SO_2, S, and SO_4 coexist on the metal. The SO_x species decompose or desorb at temperatures below 300 K. Mo(110) displays a chemical activity much larger than that observed for SO_2 on late-transition metals such as Pt(111),[8] Rh(111),[10] and Ru(001).[7] In contrast to the behavior of metallic Mo, we find that polycrystalline surfaces of MoO_2 exhibit a very low reactivity toward SO_2. A SO_2 dose of 20 L at 300 K produced only a very small coverage of Mo-bonded atomic S ($\theta_S \approx 0.05$ ML) and no adsorbed SO_x species on MoO_2. Dosing at 100 K led to the formation of a small amount of SO_4 on the oxide. This is consistent with the type of behavior seen after dosing SO_2 to oxides of other early-transition metals (TiO_2,[21] V_2O_3,[24] V_2O_5[25]), where SO_2 exposures larger than 500 L are necessary in order to produce substantial coverages of S and SO_x species. Thus, when dealing with the adsorption of SO_2 on the Cs/MoO_2

TABLE 1: Adsorption of SO_2 on ZnO and Cs/ZnO Clusters

	Geometry				adsorption energy (kcal/mol)[b]
	X_1-S(Å)[a]	X_1-O(Å)	S−O(Å)	O−S−O(Å)	
free SO_2			1.42	118	
on $Zn_{13}O_{13}(0001)-Zn$					
η^1-S a-top Zn_1	2.40		1.42	118	4
η^2-O,O a-top Zn_1		2.15	1.43	119	7
on $Cs/Zn_{13}O_{13}(0001)$					
η^1-S a-top Cs	3.26		1.48	120	19
η^2-O,O a-top Cs		3.03	1.53	124	31
on $Zn_{13}O_{13}(000\bar{1})-O$					
η^1-S a-top $O_{1'}$	1.54		1.41	119	28
on $Cs/Zn_{13}O_{13}(000\bar{1})$					
η^1-S a-top Cs	3.28		1.47	120	15
η^2-O,O a-top Cs		3.04	1.49	122	22
η^1-S a-top $O_{1'}$[c]	1.51		1.48	122	34

[a] X_1 is equal to Zn_1 in $Zn_{13}O_{13}(0001)-Zn$, Cs in $Cs/Zn_{13}O_{13}(0001)$, $O_{1'}$ in $Zn_{13}O_{13}(000\bar{1})-O$, and Cs or $O_{1'}$ in $Cs/Zn_{13}O_{13}(000\bar{1})$. [b] A positive value denotes an exothermic process. [c] Also bonded to the Cs adatom (Cs−S = 3.21 Å). In this case, the molecular plane of SO_2 and the $S-O_{1'}$ bond were tilted 41°with respect to the surface normal. In all the other adsorption cases, the molecular plane of SO_2 was parallel to the surface normal.

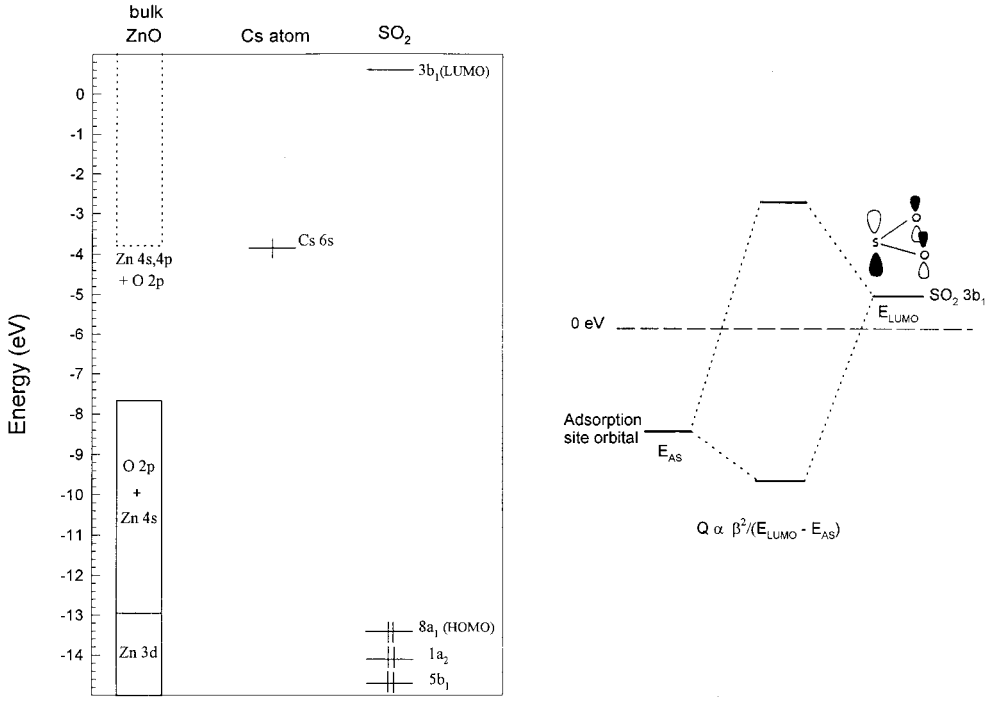

Figure 7. Left panel: Energy range covered by the bands of ZnO.[67] The empty and occupied states are indicated by dotted and solid lines, respectively. For comparison, we also indicate the energy for the 6s orbital of atomic Cs[68] and the MOs of SO_2. Right panel: Bonding interactions between the LUMO of SO_2 and an occupied orbital of the adsorption site.

systems, one is examining the effects of cesium on an oxide surface that is more or less inert.[72]

Figures 8 and 9 display Mo and Cs 3d XPS spectra recorded after depositing cesium on a MoO_2 film. The film was prepared by heavy oxidation of a Mo(110) substrate.[38] The spectrum at the bottom of Figure 8 contains, besides the features of metallic Mo, MoO_2 features with the Mo $3d_{5/2}$ peak at a binding energy of 229.2 eV.[73] The relative intensity of the MoO_2/Mo signals indicates that the oxide film is roughly 5−6 layers in thickness.[74] After the deposition of 0.6 ML of Cs at 300 K, there is a clear decrease in the relative intensity of the signal for MoO_2 (and an increase in the relative signal for Mo) that suggests that part of the oxygen is being shared by molybdenum and cesium. The Cs $3d_{5/2}$ features in Figure 9 show that the alkali disappears from the surface upon annealing to high temperature. The desorption of cesium is accompanied by an increase in the relative intensity of the Mo $3d_{5/2}$ peak for MoO_2 ($CsMoO_x \rightarrow Cs_{gas} + MoO_2$). As happens for other similar systems (Cs/ZnO,[54] Cs/TiO_2,[55] Cs/Al_2O_3[56]) the alkali desorbs from the oxide in a very broad range of temperatures. At 1050 K, ∼0.1 ML of Cs remained on the MoO_2 film.

The XPS results in Figures 8 and 9 indicate that the MoO_2 ↔ Cs interactions are very strong. These, however, do not prevent cesium from promoting or enhancing the rate of adsorption of SO_2 on MoO_2. Figure 10 shows S 2p spectra taken after exposing pure MoO_2 (bottom panel) and a MoO_2 surface precovered with 0.2 ML of Cs ($Cs_{0.2}/MoO_2$, top panel) to SO_2 at 300 K. A dose of 0.2 L to pure MoO_2 produced no detectable signal in the S 2p region. On the other hand, on the $Cs_{0.2}/MoO_2$ system a clear signal is seen for S atoms bonded to Mo (164−162 eV)[9]

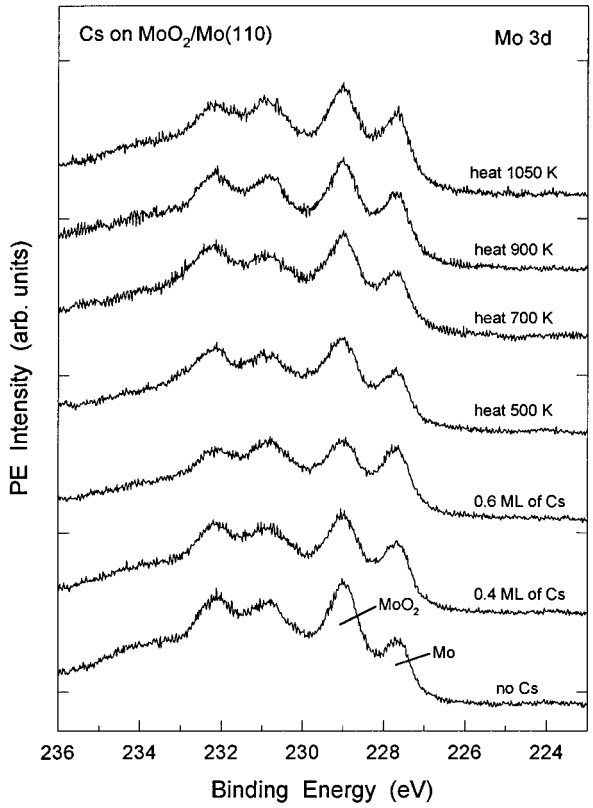

Figure 8. Mo 3d XPS spectra for the deposition of cesium on a MoO_2 film at 300 K, with subsequent annealing to high temperatures The spectra were acquired using Mg Kα radiation.

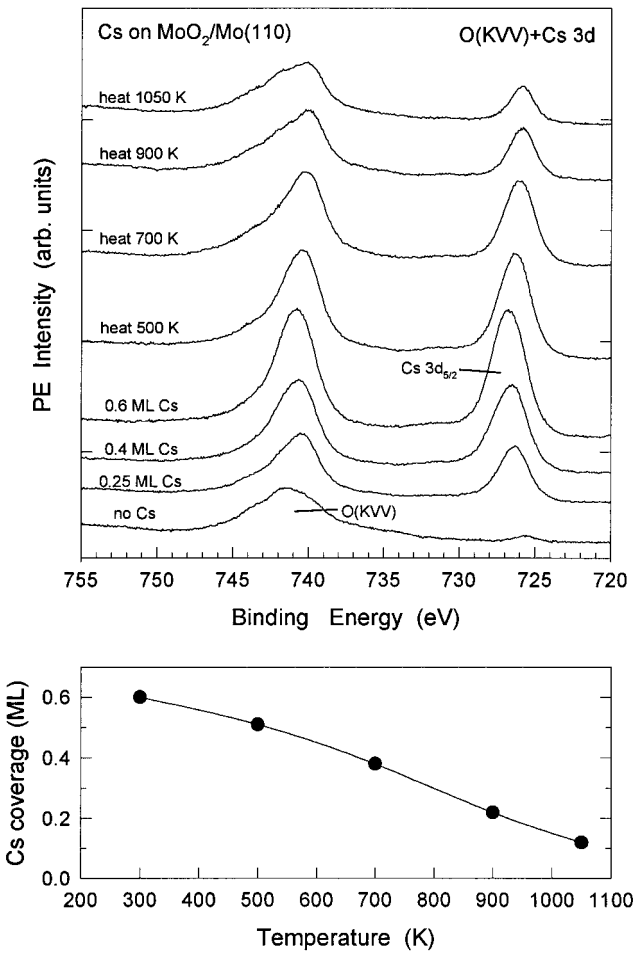

Figure 9. Top: O(KVV) Auger and Cs 3d XPS spectra for the deposition of cesium on MoO_2 at 300 K followed by annealing to high temperatures. Bottom: Variation of the coverage of Cs (i.e., Cs $3d_{5/2}$ signal, see section 2.1) with annealing temperature. The spectra were taken employing Mg Kα radiation.

and Cs (159.5−161.5 eV). Additional dosing of SO_2 leads to the formation of SO_4 on the surface. The SO_4 must be bonded to Cs, because this species decomposes on Mo(110)[9] and MoO_2 at temperatures below 300 K. After a dose of 2 L, SO_4 is the dominant species on the surface. Heating to high temperatures (300 K → 500 K → 700 K) induces the disappearance of the S 2p signals for Cs-bonded S and SO_4 without producing significant changes in the coverage of the alkali (see Figure 11). Overall, the photoemission data in Figure 10 shows that $Cs_{0.2}/MoO_2$ interacts much more strongly with SO_2 than pure MoO_2.

In Figure 12 we compare the total sulfur uptake ($S + SO_2 + SO_4$) of MoO_2, $Cs_{0.2}/MoO_2$, and $Cs_{0.6}/MoO_2$ surfaces exposed to SO_2 at 300 K. It is clear that Cs promotes the rate of adsorption of SO_2. The larger the coverage of cesium, the larger the amount of sulfur adsorbed. In the SO_2/MoO_2 systems, SO_2 interacts mainly with the supported alkali atoms. But the behavior observed for the signal of Mo-bonded S (for example see Figure 10) indicates that in some way cesium also promotes Mo ↔ SO_2 interactions. The differences in the reactivity of MoO_2 and Cs/MoO_2 can be explained using a diagram similar to that shown in Figure 7 and the simple model based on orbital mixing and perturbation theory[70,71] described above. The Cs 6s orbital is expected to be much less stable than occupied states in the valence band of MoO_2.[9] Therefore, according to eq 3, a Cs/MoO_2 system should interact more strongly with SO_2 than MoO_2. In addition, cesium weakens the Mo ↔ O interactions in MoO_2 (see Figure 8), increasing in this way the electron density on the Mo cations and their ability to respond to the presence of SO_2.

4. Discussion

4.1. Interaction of SO_2 with Metallic Cesium. Our results indicate that the chemistry of SO_2 on pure metallic cesium is rich. This is consistent with the results of previous works that in general show that the alkali has a large chemical affinity for sulfur-containing molecules: S_2,[42a] H_2S,[42a] thiophene (C_4H_4S),[75] and CH_3SH.[75] S_2, SO_2, and thiophene have low-lying unoccupied orbitals[7,10,42a,76] to which cesium can donate electrons in an easy way. This favors the formation of strong adsorption bonds and the decomposition of these adsorbates.

Cesium is more reactive toward SO_2 than late-transition metals such as Rh, Ni, Pd, Pt, Cu, and Ag that do not dissociate the molecule or induce the formation of SO_3/SO_4 species at 100 K.[3−6,8,10] In part this can be attributed to the fact that metallic cesium has a much lower work function than late-transition metals,[77] making easier metal → SO_2(LUMO) electron transfers. Mo and Ru are able to dissociate SO_2 at 100 K,[7,9] but on these metals one sees saturation coverages of S, O, and SO_x species that are at the submonolayer level. This is not the case on cesium, where total sulfur coverages well above a monolayer are relatively easy to produce and the sulfur species penetrate into the bulk of the sample. This phenomenon is made possible by the combination of two factors. First, the thermochemical stability of cesium sulfites and sulfates is very large[64] and second, the cohesive energy of metallic cesium is so low (18.5 kcal/mol)[78] that the potential barrier for the penetration of S, O, and SO_x into the bulk of the metal is probably very small. Similar arguments have been used to explain the vigorous reaction of SO_2 with metallic zinc.[27]

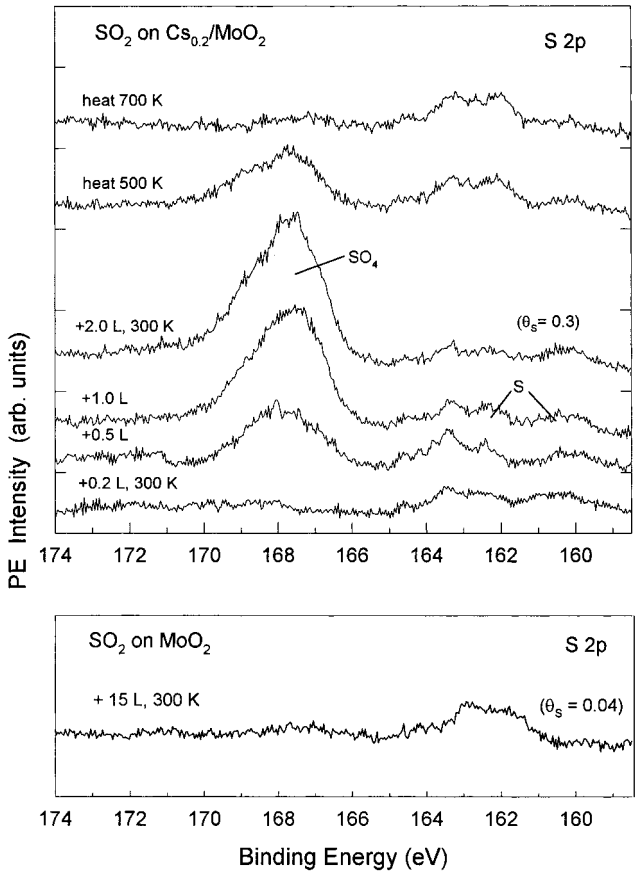

Figure 10. Top: S 2p spectra for the reaction of SO_2 with a MoO_2 surface precovered by 0.2 ML of cesium. Sulfur dioxide was dosed at 300 K and the sample was then annealed to 500 and 700 K. Bottom: S 2p spectrum obtained after dosing 15 L of SO_2 to a pure MoO_2 surface at 300 K. All the spectra were acquired using a photon energy of 260 eV.

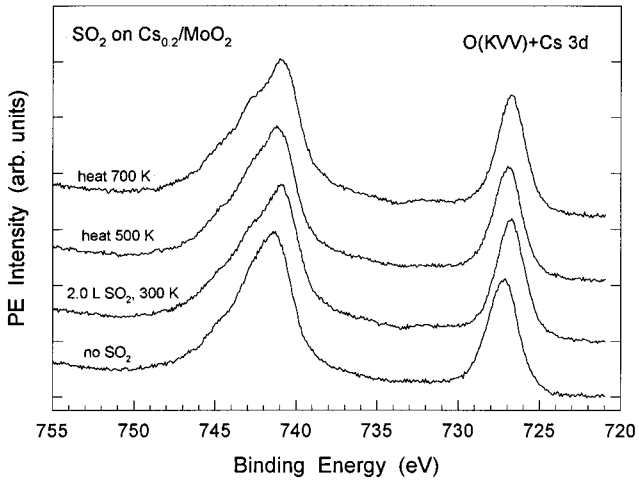

Figure 11. O(KVV) Auger and Cs 3d XPS spectra recorded in the same set of experiments that produced the S 2p spectra in the top panel of Figure 10: SO_2 on $Cs_{0.2}/MoO_2$. The electrons were excited using Mg Kα radiation.

4.2 Interaction of SO_2 with Cs/ZnO and Cs/MoO_2. In principle, when an alkali overlayer interacts with an oxide support one can have two limiting cases.[31] The first is adsorption of the alkali on narrow band gap (E_{gap}) oxides ($E_{gap} < 4$ eV), in which the cations can be reduced to lower oxidation states by some alkalis and for which charge transfer from the alkali to the oxide is reported to be energetically favorable.[30,31] In this case, one can expect large changes in the chemical properties

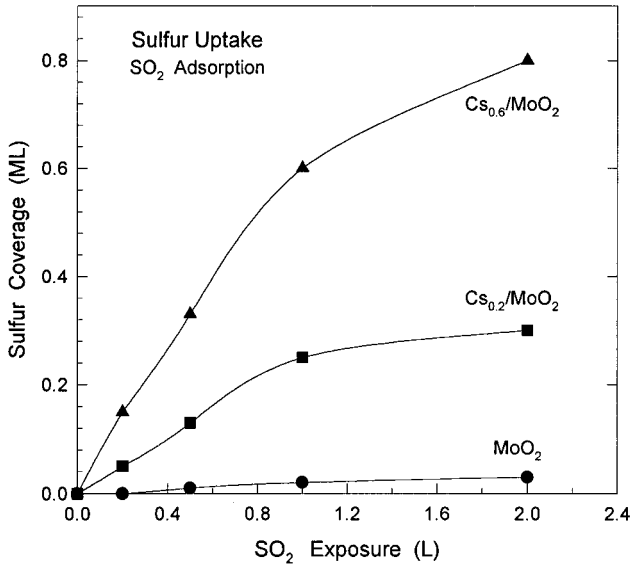

Figure 12. Total amount of sulfur (SO_4 + SO_2 + S) deposited on pure MoO_2, $Cs_{0.2}/MoO_2$, and $Cs_{0.6}/MoO_2$ after several doses of SO_2 at 300 K. The coverage of sulfur was determined by measuring the area under the S 2p features (see section 2.1).

of the alkali and oxide. The second case corresponds to adsorption onto wide band gap oxides ($E_{gap} > 5$ eV), where the overlayer → support charge transfer is expected to be small.[30,31] Here, the bonding energies are weak and controlled by interactions of the alkali with vacancies and defect sites of the oxide surface.[30,31] In this case, one can expect relatively small perturbations in the chemical properties of the supported alkali. The systems under study in this work involve oxides that have a narrow band gap,[79] and the Cs ↔ ZnO and Cs ↔ MoO_2 interactions are very strong. Despite this, one finds that the supported Cs atoms remain very reactive toward SO_2. On the alkali adatoms the chemistry is as complex as seen on pure metallic cesium (coexistence of S, SO_2, and SO_4). This is valid even at low coverages (0.1−0.2 ML) of cesium when the adatoms are in a highly ionic state ($Cs^{\delta+}$).

In a recent work, the adsorption of SO_2 on sodium-impregnated alumina was examined using infrared spectroscopy.[18a] It was found that at low sodium coverages the alkali acts as a promoter for the formation of adsorbed sulfites and sulfates which may have structures similar to those of aluminum sulfite and sulfate, respectively. At high Na coverage, evidence was found for the existence of SO_3/SO_4 species bonded to the alkali.[18a] Our results for the Cs/ZnO and Cs/MoO_2 systems show that the alkali promotes the formation of sulfate groups on the oxide surface. In the case of Cs/MoO_2, the SO_4 is mainly associated with the alkali adatoms (clearly the "active phase", see Figure 10) because the oxide support has a very low chemical activity. On the other hand, for Cs/ZnO, the SO_4 may be bonded to the admetal and/or oxide substrate (one finds S 2p features that match those of Cs- and ZnO-bonded SO_4, see Figure 4). In the Cs/ZnO and Cs/MoO_2 systems, the alkali promotes the full decomposition of SO_2 and the deposition of atomic sulfur on the surface. This can be useful in catalytic processes employed for the removal or destruction of sulfur dioxide:[1b,17] $2CO + SO_2 \rightarrow 2CO_2 + S_{solid}$; or $2H_2S + SO_2 \rightarrow 2H_2O + 3S_{solid}$ (Claus process).

In the chemical industry, zinc oxide is used as a sorbent for SO_2 and other sulfur-containing molecules.[1b,80] We have found that cesium substantially increases the rate of adsorption of SO_2, S_2,[42a] H_2S,[42a] and thiophene[75] on ZnO surfaces. Thus, doping with cesium is a good route for enhancing the performance of

zinc oxide as a sorbent. Cu/ZnO catalysts are widely used for the synthesis of alcohols from CO/CO_2 mixtures, the water−gas shift reaction ($CO + H_2O \rightarrow CO_2 + H_2$), and methanol−steam reforming ($CH_3OH + H_2O \rightarrow CO_2 + 3H_2$).[17a,b,30] Cesium is added to the Cu/ZnO catalysts to improve their activity and/or selectivity.[17a,b,81] The Cu/ZnO catalysts are readily poisoned by sulfur-containing molecules that are present at ppm levels in oil-derived feedstocks.[17a,b] The present results indicate that in this respect the effects of cesium should be negative, since the alkali probably accelerates sulfur poisoning.

5. Conclusions

(1) Metallic cesium reacts vigorously with SO_2 at temperatures between 100 and 300 K. At 100 K, the amount of SO_2 that fully dissociates ($SO_{2,gas} \rightarrow S_a + 2O_a$) on the alkali metal is relatively small, and SO_x ($x = 2-4$) species predominate on the surface. At room temperature the stability of the $CsSO_x$ species is lower than at 100 K, and the formation of CsO_y and CsS_y becomes important.

(2) In the Cs/ZnO and Cs/MoO_2 systems, the alkali ↔ oxide interactions are very strong. Despite of this, the supported Cs atoms retain a large chemical affinity for SO_2 and are able to enhance the rate of adsorption of the molecule on the oxide surfaces. The larger the coverage of Cs on ZnO and MoO_2, the faster the rate of adsorption of SO_2, and the larger the amount of S and SO_x ($x = 2-4$) species present on the surface.

(3) At 300 K, sulfur dioxide preferentially interacts with the O sites of ZnO forming SO_4 groups on the surface. In contrast for Cs/ZnO, SO_2 reacts with the metal adatoms and, in addition to SO_4, SO_2, and S, are also present on the surface. The Cs adatoms provide occupied states that are very efficient for bonding interactions with the LUMO of SO_2. Cs atoms supported on Zn-terminated terraces of ZnO respond much more strongly to the presence of SO_2 than Cs atoms supported on O-terminated terraces. The bonding interactions between the ZnO(0001)−Zn face and SO_2 are weak, and promotion with Cs adatoms considerably improves the energetics for SO_2 adsorption.

(4) MoO_2 has a relatively low reactivity toward SO_2. For this oxide, cesium induces drastic increases in the rate of adsorption of SO_2. On one hand, cesium weakens the Mo ↔ O interactions in MoO_2 enhancing the chemical affinity of the Mo cations for SO_2. But, even after these changes, SO_2 preferentially reacts with the supported cesium atoms.

Acknowledgment. This work was carried out at Brookhaven National Laboratory and supported by the U.S. Department of Energy, Chemical Science Division (DE-AC02-98CH10886). The NSLS is supported by the divisons of Materials and Chemical Sciences of the U.S. Department of Energy. T.J. acknowledges the support of a NATO grant awarded in 1997.

References and Notes

(1) (a) Stern, A. C.; Boubel, R. W.; Turner, D. B.; Fox, D. L. *Fundamentals of Air Pollution*, 2nd ed; Academic Press: Orlando, 1984. (b) Slack, A. V.; Hollinden, G. A. *Sulfur Dioxide Removal from Waste Gases*, 2nd ed; Noyes Data Corporation: Park Ridge, NJ, 1975.

(2) (a) Taylor, K. C. *Catal. Rev. Sci. Eng.* **1993**, *35*, 457. (b) McCabe, R. W.; Usmen, R. K. *Studies in Surf. Sci. and Catal.* **1996**, *101*, 355. (c) Beck, D. D.; Sommers, J. W.; DiMaggio, C. L. *Appl. Catal. B* **1994**, *3*, 205.

(3) (a) Ahner, J.; Effendy, A.; Wassmuth, H. W. *Surf. Sci*. **1992**, *269/270*, 372. (b) Ahner, J.; Wassmuth, H. W. *Surf. Sci*. **1993**, *287/288*, 125. (c) Polčik, M.; Wilde, L.; Haase, J. *Phys. Rev. B* **1998**, *57*, 1868. (d) Polčik, M.; Wilde, L.; Haase, J.; Brena, B.; Cocco, D.; Comelli, G.; Paolucci, G. *Phys. Rev. B* **1996**, *53*, 13720. (e) Nakahashi, T.; Hamamatsu, H.; Terada, S.; Sakano, M.; Matsui, F.; Yokoyama, T.; Kitajima, Y.; Ohta, T. *J. Phys. IV France* **1997**, *C2*, 679. (f) Pangher, N.; Wilde, L.; Polčik, M.; Haase, J. *Surf. Sci.* **1997**, *372*, 211. (g) Nakahashi, T.; Terada, S.; Yokoyama, T.; Hamamatsu, H.; Kitajima, Y.; Sakano, M.; Matsui, F.; Ohta, T. *Surf. Sci*. **1997**, *373*, 1 (h) Leung, K. T.; Zhang, X. S.; Shirley, D. A. *J. Phys. Chem*. **1989**, *93*, 6164. (i) Sun, Z. L.; White, J. M. *J. Phys. Chem*. **1994**, *98*, 4641. (j) Pressley, L. A.; Kiss, J.; White, J. M.; Castro, M. E. *J. Phys. Chem*. **1993**, *97*, 902. (k) Castro, M. E.; White, J. M. *J. Chem. Phys*. **1991**, *95*, 6057. (l) Ahner, J.; Effendy, A.; Vajen, K.; Wassmuth, H. W. *Vacuum* **1990**, *41*, 98. (m) Sosa, A. G.; Walsh, J. F.; Muryn, C. A.; Finetti, P.; Thornton, G.; Robinson, A. W.; D'Addato, S.; Frigo, S. P. *Surf. Sci*. **1996**, *364*, L519. (n) Solomon, J. L.; Madix, R. J.; Wurth, W.; Stöhr, J. *J. Phys. Chem*. **1991**, *95*, 3687. (o) Höfer, M.; Stolz, H.; Wassmuth, H. W.; *Surf. Sci*. **1993**, *287/288*, 130.

(4) (a) Höfer, M.; Stolz, H.; Wassmuth, H. W. *Surf. Sci*. **1992**, *272*, 342. (b) Polčik, M.; Wilde, L.; Haase, J.; Brena, B.; Comelli, G.; Paolucci, G. *Surf. Sci*. **1997**, *381*, L568. (c) Wilson, K.; Hardacre, C.; Baddeley, C. J.; Lüdecke, J; Woodruff, D. P.; Lambert, R. M. *Surf. Sci*. **1997**, *372*, 279. (d) Wilson, K.; Hardacre, C.; Lambert, R. M. *J. Phys. Chem*. **1995**, *99*, 13755. (e) Sun, Y. M.; Sloan, D.; Alberas, D. J.; Kovar, M.; Sun, Z. J.; White, J. M. *Surf. Sci*. **1994**, *319*, 34. (f) Höfer, M.; Hillig, S.; Wassmuth, H. W. *Vacuum* **1990**, *41*, 102. (g) Köhler, U.; Wassmuth, H. W. *Surf. Sci*. **1983**, *126*, 448. (h) Astegger, St.; Bechtold, E. *Surf. Sci*. **1982**, *122*, 491. (i) Köhler, U.; Wassmuth, H. W. *Surf. Sci*. **1982**, *117*, 668. (j) Katekaru, J. Y.; Garwood, G. A.; Hershberger, J. F., Jr.; Hubbard, A. T. *Surf. Sci*. **1982**, *121*, 396. (k) Zebisch, P.; Stichler, M.; Trischberger, P.; Weinelt, M.; Steinrück, H. P. *Surf. Sci*. **1997**, *371*, 235.

(5) (a) Zebisch, P.; Weinelt, M.; Steinrück, H. P. *Surf. Sci*. **1993**, *295*, 295. (b) Terada, S.; Imanishi, A.; Yokoyama, T.; Takenaka, S.; Kitajima, Y.; Ohta, T. *Surf. Sci*. **1995**, *336*, 55. (c) Terada, S.; Imanishi, A.; Yokoyama, T.; Kitajima, Y.; Ohta, T. *J. Electron. Spec. Relat. Phenom*. **1996**, *80*, 245. (d) Jackson, G. J.; Lüdecke, J.; Driver, S. M.; Woodruff, D. P.; Jones, R. G.; Chan, A.; Cowie, B. C. C. *Surf. Sci*. **1997**, *389*, 223. (e) Yokoyama, T.; Terada, S.; Yagi, S.; Imanishi, A.; Takenaka, S.; Kitajima, Y.; Ohta, T. *Surf. Sci*. **1995**, *324*, 25. (f) Yokoyama, T.; Terada, S.; Imanishi, A.; Kitajima, Y.; Kosugi, N.; Ohta, T. *J. Electron. Spec. Relat. Phenom*. **1996**, *80*, 161. (g) Yokoyama, T.; Imanishi, A.; Terada, S.; Namba, H.; Kitajima, Y.; Ohta, T. *Surf. Sci*. **1995**, *334*, 88. (h) Burke, M. L.; Madix, R. J. *Surf. Sci*. **1988**, *194*, 223. (i) Gainey, T. C.; Hopkins, B. J. *J. Phys. C: Solid State Phys*. **1983**, *16*, 975. (j) Tournas, A. D.; Potts, A. W. *J. Electron. Spec. Relat. Phenom*. **1995**, *73*, 231.

(6) (a) Haase, J. *J. Phys.: Condens. Matter* **1997**, *9*, 3647 (b) Sellers, H.; Shustorovich, E. *J. Mol. Catal. A: Chemical* **1997**, *119*, 367.

(7) Jirsak, T.; Rodriguez, J. A; Chaturvedi, S.; Hrbek, J. *Surf. Sci.* **1998**, *418*, 8.

(8) Rodriguez, J. A.; Jirsak, T.; Chaturvedi, S.; Hrbek, J. *J. Am. Chem. Soc*. **1998**, *120*, 11149.

(9) Jirsak, T.; Rodriguez, J. A.; Hrbek, J. *Surf. Sci.* **1998**, *418*, 8.

(10) Rodriguez, J. A.; Jirsak, T.; Chaturvedi, S. *J. Chem. Phys.* **1999**, *110*, 3138.

(11) Sakaki, S; Sato, H.; Imai, Y.; Morokuma, K.; Ohkubo, K. *Inorg. Chem.* **1985**, *24*, 4538.

(12) Pacchioni, G.; Clotet, A.; Ricart, J. M. *Surf. Sci.* **1994**, *315*, 337.

(13) Rodriguez, J. A.; Chaturvedi, S.; Jirsak, T.; Hrbek, J. *J. Chem. Phys.* **1998**, *109*, 4052.

(14) (a) L'Argentière, P. C.; Cañon, M. M.; Fìgoli, N. S.; Ferron, J. *Appl. Surf. Sci.* **1993**, *68*, 41. (b) L'Argentière, P. C.; Cañon, M. M.; Fìgoli, N. S. *Appl. Surf. Sci*. **1995**, *89*, 63.

(15) (a) Tschöpe, A.; Liu, W.; Flytzani-Stephanopoulos, M.; Ying, J. Y. *J. Catal.* **1995**, *157*, 42. (b) Liu, W.; Sarofim, A. F.; Flytzani-Stephanopoulos, M. *Appl. Catal. B* **1994**, *4*, 167. (c) Liu, W.; Flytzani-Stephanopoulos, M. In *Environmental Catalysis*, ACS Symposium Series 552; American Chemical Society: Washington, DC, 1994; Chapter 31, p 375.

(16) (a) Waqif, M.; Saur, O.; Lavalley, J. C.; Perathoner, S.; Centi, G. *J. Phys. Chem.* **1991**, *95*, 4051. (b) Centi, G.; Passarini, N.; Perathoner, S.; Riva, A. *Ind. Eng. Chem. Res.* **1992**, *31*, 1947.

(17) (a) Thomas, J. M.; Thomas, W. J. *Principles and Practices of Heterogeneous Catalysis*; VHC: New York, 1997. (b) *Handbook of Heterogeneous Catalysis*; Ertl, G.; Knözinger, H.; Weitkamp, J., Eds.; Wiley-VCH: New York, 1997. (c) *Handbook of Pollution Control Processes*; Noyes, R., Ed.; Noyes Data Corporation: Park Ridge, NJ, 1991.

(18) (a) Mitchell, M. B.; Sheinker, V. K.; White, M. G. *J. Phys. Chem.* **1996**, *100*, 7550. (b) Rao, S. N. R.; Waddell, E.; Mitchell, M. B.; White, M. G. *J. Catal.* **1996**, *163*, 176.

(19) (a) Town, J. W.; Paige, J. I.; Russell, J. H. *Chem. Eng. Prog., Symp. Ser.* **1970**, *105*, 260. (b) Deo, A. V.; Dalla Lana, I. G.; Habgood, H. W. *J. Catal.* **1971**, *21*, 270.

(20) (a) Gavalas, G. R.; Edelstein, S.; Flytzani-Stephanopoulos, M.; Weston, T. A. *AIChe J.* **1987**, *33*, 258. (b) Ma, W. T.; Haslbeck, J. L. *Environ. Prog.* **1993**, *12*, 163. (c) Chung, J. S.; Paik, S. C.; Kim, H. S.; Lee, D. S.; Nam, I. S. *Catal. Today* **1997**, *35*, 37.

(21) (a) Smith, K. E.; Mackay, J. L.; Henrich, V. E. *Phys. Rev. B* **1987**, *35*, 5822. (b) Onishi, H.; Aruga, T.; Egawa, C.; Iwasawa, Y. *Surf. Sci*. **1988**, *193*, 33.

(22) Smith, K. E.; Henrich, V. E. *Phys. Rev. B* **1985**, *32*, 5384.

(23) Kurtz, R.; Henrich, V. E. *Phys. Rev. B* **1987**, *36*, 3413.

(24) Smith, K. E.; Henrich, V. E. *Surf. Sci.* **1990**, *225*, 47.

(25) Zhang, Z.; Henrich, V. E. *Surf. Sci*. **1994**, *321*, 133.
(26) Li, X.; Henrich, V. E. *Phys. Rev. B* **1993**, *48*, 17486.
(27) Chaturvedi, S.; Rodriguez, J. A.; Jirsak, T; Hrbek, J. *J. Phys. Chem. B* **1998**, *102*, 7033.
(28) (a) Wilson, K.; Lee, A. F.; Hardacre, C.; Lambert, R. M. *J. Phys. Chem. B* **1998**, *102*, 1736. (b) Dalla Lana, I. G.; Karge, H. G.; George, Z. M. *J. Phys. Chem*. **1993**, *97*, 8005. (c) Yao, H. C.; Stephien, H. K.; Gandhi, H. S. *J. Catal*. **1981**, *67*, 231.
(29) Babaeva, M. A.; Tsyganeko, A. A.; Filiminov, V. N. *Kinet. Catal*. **1984**, *25*, 787.
(30) Campbell, C. T. *Surf. Sci. Rep*. **1997**, *27*, 1.
(31) Madey, T. E.; Yakshinsky, B. V.; Ageev, V. N.; Johnson, R. E. *J. Geophys. Res.* **1998**, *103*, 5873.
(32) Williams, G. P. *Electron Binding Energies of the Elements, Version II*; National Synchrotron Light Source, Brookhaven National Laboratory, 1992.
(33) Goodman, D. W. *Chem. Rev*. **1995**, *95*, 523.
(34) Freund, H-J.; Kulenbeck, H.; Staemmler, V. *Rep. Prog. Phys.* **1996**, *59*, 283.
(35) Chaturvedi, S.; Rodriguez, J. A.; Hrbek, J. *J. Phys. Chem. B.* **1997**, *101*, 10860.
(36) Chaturvedi, S.; Rodriguez, J. A.; Hrbek, J. *Surf. Sci*. **1997**, *384*, 260.
(37) Rodriguez, J. A.; Hrbek, J. *J. Vac. Sci. Technol. A* **1994**, *12*, 2140.
(38) (a) Wu, G.; Bartlett, B.; Tysoe, W. T. *Langmuir* **1998**, *14*, 1435. (b) H. M. Kennett, H. M.; Lee, A. E. *Surf. Sci.* **1975**, *48*, 591 and 624. (c) Bartlett, B.; Scheerson, V. L.; Tysoe, W. T. *Catal. Lett.* **1995**, *3*, 1.
(39) (a) Gorodetsky, D. A.; Melnik, Y. P.; Usenko, V. A.; Yas'ko, A. A.; Yarigin, V. I. *Surf. Sci.* **1994**, *315*, 51. (b) Soukiassian, P.; Roubin, P.; Cousty, J.; Riwan, R.; Lecante, J. *J. Phys. C* **1985**, *18*, 4785.
(40) (a) Sanchez, A.; De Miguel, J. J.; Martinez, E.; Miranda, R. *Surf. Sci.* **1986**, *171*, 157. (b) Peralta, L.; Berthier, Y.; Oudar, J. *Surf. Sci.* **1976**, *55*, 199.
(41) Dupuis, M.; Chin, S.; Marquez, A. In *Relativistic and Electron Correlation Effects in Molecules and Clusters*; Malli, G. L., Ed; NATO ASI Series; Plenum: New York, 1992.
(42) (a) Rodriguez, J. A.; Jirsak, T.; Chaturvedi, S.; Hrbek, J. *Surf. Sci*. **1998**, *407*, 171. (b) Rodriguez, J. A.; Chaturvedi, S.; Kuhn, M.; Hrbek, J. *Phys. Chem. B* **1998**, *102*, 5511.
(43) (a) Hay, P. J.; Wadt, W. R. *J. Chem. Phys*. **1985**, *82*, 270. (b) Wadt, W. R.; Hay, P. J. *J. Chem. Phys.* **1985**, *82*, 284.
(44) Rodriguez, J. A.; Kuhn, M. *J. Phys. Chem.* **1996**, *100*, 381.
(45) Stevens, W. J.; Basch, H.; Krauss, M. *J. Chem. Phys.* **1984**, *81*, 6026.
(46) (a) Whitten, J. L.; Yang, H. *Surf. Sci. Rep.* **1996**, *24*, 55. (b) van Santen, R. A.; Neurock, M. *Catal.-Rev.-Sci. Eng*. **1995**, *37*, 557.
(47) *Quantum Chemistry Approaches to Chemisorption and HeterogeneousCatalysis*; Ruette, F., Ed.; Kluwer: Dordtrecht, 1992.
(48) Mullins, D. R.; Lyman, P. F.; Overbury, S. H. *Surf. Sci.* **1992**, *277*, 64.
(49) Küppers, J.; Ertl, G. *Surf. Sci.* **1978**, *77*, L647.
(50) In ref 28a, a difference of 5−5.5 eV is observed between the S 2p binding energies of S and SO_4 on alumina. A separation of ∼5 eV is reported in ref 4b for the S $2p_{3/2}$ binding energies of S and SO_4 on Pt(111), whereas a difference of ∼3 eV is observed between the S $2p_{3/2}$ binding energies of chemisorbed S and SO_2.
(51) Hrbek, J.; Yang, Y. W.; Rodriguez, J. A. *Surf. Sci*. **1993**, *296*, 164.
(52) Egelhoff, W. F. *Surf. Sci. Rep.* **1987**, *6*, 253.
(53) (a) Rodriguez, J. A.; Kuhn, M.; Hrbek, J. *Chem. Phys. Lett*. **1996**, *251*, 13. (b) Hrbek, J.; Li, S. Y.; Rodriguez, J. A.; van Campen, D. G.; Huang, H. H.; Xu, G.-Q. *Chem. Phys. Lett.* **1997**, *267*, 65.
(54) Chaturvedi, S.; Rodriguez, J. A. *Surf. Sci.* **1998**, *401*, 282.
(55) Grant, A.; Campbell, C. T. *Phys. Rev. B* **1997**, *55*, 1844.
(56) Rodriguez, J. A.; Kuhn, M.; Hrbek, J. *J. Phys. Chem.* **1996**, *100*, 18240.
(57) (a) Rodriguez, J. A.; Campbell, C. T. *J. Phys. Chem.* **1987**, *91*, 6648. (b) Rodriguez, J. A. *Surf. Sci.* **1989**, *222*, 383. (c) Rodriguez, J. A. *Langmuir* **1988**, *4*, 1006. (d) Anderson, A. B.; Nichols, J. A. *J. Am. Chem. Soc.* **1986**, *108*, 4742. (e) Sekine, R.; Adachi, H.; Morimoto, T. *Surf. Sci.* **1989**, *208*, 177.
(58) Abrahams, S. C.; Berstein, J. L. *Acta Crystallogr. B* **1969**, *25*, 1223.
(59) Leysen, R.; Hopkins, B. J.; Taylor, P. A. *J. Phys. C: Solid State Phys.* **1975**, *8*, 907.
(60) Purdie, D.; Muryn, C. A.; Crook, S.; Wincott, P. L.; Thornton, G.; Fischer, D. A. *Surf. Sci.* **1993**, *290*, L680.
(61) (a) The charges were calculated using a Mulliken population analysis.[61b] Due to the limitations of this type of analysis,[61c] the charges must be interpreted only in qualitative terms. (b) Mulliken, R. S. *J. Chem. Phys.* **1955**, *23*, 1841. (c) Szabo, A.; Ostlund, N. S. *Modern Quantum Chemistry*; McGraw-Hill: New York, 1989.
(62) Sellers, H.; Shustorovich, E. *Surf. Sci.* **1996**, *346*, 322.
(63) Sellers, H.; Shustorovich, E. *Surf. Sci.* **1996**, *356*, 209.
(64) *Lange's Handbook of Chemistry*, 13th ed.; Dean, J., Ed.; McGraw-Hill: New York, 1985; Table 9-1.
(65) Nimlos, M. R.; Ellison, G. B. **1986**, *90*, 2574.
(66) (a) Mingos, D. M. P. *Transition Met. Chem.* **1978**, *3*, 1. (b) Shenk, W. A. *Angew. Chem., Int. Ed. Engl.* **1987**, *26*, 98.
(67) (a) The energy positions for the bands of ZnO were calculated using photoemission data[67b,c] and reported values for the band gap and work function of the oxide.[67b] (b) Henrich, V. E.; Cox, P. A. *The Surface Chemistry of Metal Oxides*; University Press: Cambridge, 1994. (c) Solomon, E. I.; Jones, P. M.; May, J. A. *Chem. Rev.* **1993**, *93*, 2623.
(68) (a) The energy for the Cs 6s orbital was estimated using the corresponding experimental ionization potential for atomic Cs (3.9 eV).[68b] Our SCF calculations predict an energy of −3.4 eV for the 6s orbital of atomic Cs. (b) Moeller, T. *Inorganic Chemistry*; Wiley: New York, 1982; p 78.
(69) In the $Cs/Zn_{13}O_{13}(0001)$ and $Cs/Zn_{13}O_{13}(000\bar{1})$ clusters, it was found that the Cs 6s orbitals were stabilized (i.e., energy more negative) by ∼1.8 and 2.3 eV with respect to the energy in free Cs.
(70) Shustorovich, E.; Baetzold, R. C. *Science* **1985**, *227*, 876.
(71) Hammer, B.; Morikawa, Y.; Nørkskov, J. K. *Phys. Rev. Lett.* **1996**, *76*, 2141.
(72) For example, this is the case when one compares the chemical activities of ZnO and MoO_2.
(73) Wagner, C. D.; Riggs, W. M.; Davis, L. E.; Moulder, J. F. *Handbook of X-ray Photoelectron Spectroscopy*; Perkin-Elmer; Eden Prairie, Minnesota, 1978; page 104.
(74) Li, S. Y.; Rodriguez, J. A.; Hrbek, J.; Huang, H. H.; Xu, G.-Q. *Surf. Sci.* **1996**, *366*, 29.
(75) In preparation.
(76) Rodriguez, J. A. *Surf. Sci.* **1992**, *278*, 326.
(77) Michaelson, H. B. *J. Appl. Phys.* **1977**, *48*, 4729.
(78) Kittel, C. *Introduction to Solid State Physics*, 6th ed.; Wiley: New York, 1986; p 55.
(79) Strehlow, W. H.; Cook, E. L. *J. Phys. Chem. Ref. Data* **1973**, *2*, 163.
(80) Satterfield, C. N. *Heterogeneous Catalysis*; McGraw-Hill: New York, 1980; p 261.
(81) Nakamura, J.; Campbell, J. M.; Campbell, C. T. *J. Chem. Soc. Faraday Trans.* **1990**, *86*, 2725, and references therein.